https://doi.org/10.2352/CIC.2025.33.1.42

Color Co-ocurrence Matrix based on color appearance model CIECAM16. Application to dermatological images

Begoña Acha*, Carmen Serrano*

****Department of Signal Theory and Communications. Escuela Técnica Superior de Ingeniería. Universidad de Sevilla, Spain, bacha@us.es, cserrano@us.es***

Abstract

New color texture features have been designed based on second-order statistics features that are calculated from a new color co-occurrence matrix (CCM). These CCM features have three main novel design aspects. First, they incorporate perceptual color differences in their computation. Second, the second-order probability distributions are based on the CIECAM16 color appearance model and its derived Uniform Color Space (CIECAM16-UCS). Third, to avoid high-dimensional and sparse cooccurrence matrices, low-dimensional CCMs are calculated using perceptual clustering for color quantization. The ability of these new CCM metrics to analyze colored textures has been validated in two experiments using biomedical color texture images: Basal Cell Carcinoma (BCC) dermoscopic pattern detection and hemangioma depth estimation from color photographs. Both experiments demonstrated that the proposed CCM features outperformed other texture analysis methods.

Introduction

Whether to include color in texture descriptors or not has been a discussed issue along texture characterization research. Some studies reflect that taking into account color information in texture description is not necessary, while others maintain that color information in texture characterization is crucial for a better description of a texture. [1]. Among the contributions that consider that color information is relevant for texture characterization, the most common way in introducing the color information is extracting the texture features to each color component separately, losing the vectorial nature of color [1].

Recently, other color texture descriptors more elaborated have been published. If we concentrate on second-order statistics and, particularly, co-ocurrence matrixes, not many contributions can be found in the literature. Chaky and Dey [2] present an interesting review of different color features. One of them is a color co-occurrence matrix (CCM), that computes the spatial color distributions features in an image. Most works devoted to calculate a CCM extract the co-occurrences of the pixels comparing one pixel belonging to a color representation channel with another pixel belonging to a different color representation channel ($CCM_{H,S}$, $CCM_{H,H}$, $CCM_{R,G}$, …, where H is hue component, S is saturation component, R is red component, G is green component). Shim and Choi [3] propose a CCM where the probabilities are calculated using only the H channel. Afterwards, this matrix was extended to generate a Modified Color Co-occurrence Matrix (MCCM) by separating the diagonal and non-diagonal components of CCM [4].

In this paper, we present a new color co-occurrence matrix (CCM) that has three main innovations compared to existing approaches: 1) it incorporates a color appearance model, making it more perceptual, 2) it calculates second-order probability distributions based on the CIECAM16 color appearance model that takes into account the vectorial nature of color, and 3) a perceptual clustering for color quantization is proposed, in order to avoid high-dimensional and sparse co-occurrence matrices. To this end, we quantify colors in CIECAM16 and redefine the distance between color pixels, considering the uniformity of the CIECAM16-UCS (Uniform Color Space) and, therefore, the perceptually correlated distances between pixels.

Contributions

New parameters extracted from a new perceptually-inspired color co-occurrence matrix have been designed. To the best of our knowledge, no other authors in the literature have considered uniform color spaces and recent advances in color appearance models for the computation of texture parameters extracted from co-occurrence matrices. Furthermore, the second-order probability distributions are estimated taking into account the vectorial nature of color.

Methodology

The computation of the proposed CCM texture metrics involves four main steps, as depicted in Figure 1. First, the color image must be transformed into a uniform color space (UCS), in which Euclidean distances are correlated to perceived color differences. *CIECAM16-UCS* has been used to this end. Second, a color clustering in this color space must be performed to reduce the number of colors to K, where K is the number of clusters. Third, a co-occurrence matrix containing an estimate of the probability of two pixels occurring in a particular relative position is calculated. Fourth, CCM features are computed from these matrices, considering perceived color differences rather than index subtraction, unlike gray-level co-occurrence matrix (GLCM). These four steps are described in the following subsections.

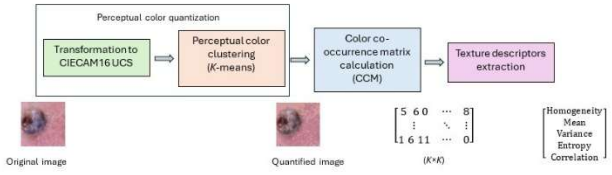

Figure 1: Steps for CCM features extraction.

Uniform color spaces

A uniform color space is a color system in which Euclidean distances correlate well with perceived color differences. In 1976, the *CIE* (Commission Internationale de l'Eclairage) standardized

two color spaces, *L*u*v** and *L*a*b**, to provide a tool for measuring color differences as perceived by human observers [5].

The appearance of colors is strongly affected by viewing conditions and the surrounding color stimuli. Therefore, it is useful to apply a color appearance model when analyzing natural images, as well as images related to specific applications, such as medical images. *CIECAM16* is a color appearance model that the CIE recently recommended as a replacement for *CIECAM02* [6].

From *CIECAM16* we can obtain the six correlates: lightness *J*, chroma *C*, hue composition *H*, hue angle *h*, colorfulness *M*, saturation *s* and brightness *Q*. From this color appearance model, a uniform color space *CIECAM16-UCS* can be defined:

$$J' = \frac{1.7J}{1+0.007J} \quad (1)$$

$$M' = \ln\frac{1+0.0228M}{0.0228} \quad (2)$$

$$a' = M'\cos(h) \quad (3)$$

$$b' = M'\sin(h) \quad (4)$$

The color difference between two samples can be computed as the Euclidean distance between them in *CIECAM16-UCS*:

$$\Delta E = [\Delta J'^2 + \Delta a'^2 + \Delta b'^2]^{1/2} \quad (5)$$

Perceptual clustering

Three-dimensional vectors can represent a large number of colors. Therefore, it is necessary to group them in order to reduce the dimensions of the CCM and avoid sparse matrices. To this end, the *K*-means algorithm [7] will be applied. *K* represents the number of centroids, i.e. the most representative colors, in the image set. The clustering will be performed in the *CIECAM16-UCS* color space.

Color Cooccurrence Matrix Estimation

One of the most important texture features used in texture analysis is those derived from the gray-level co-occurrence matrix (GLCM). The GLCM is calculated from the estimation of second-order gray-level distribution [8]. The GLCM provides the frequency with which two gray levels co-occur at a given relative location in an image, i.e., the probability of having pixel values *i* and *j* in those relative positions. To characterize texture, parameters such as homogeneity, entropy, correlation, mean, and variance are extracted from the GLCM [8].

The introduction of color information could improve the accuracy in classifying color texture [9]. A grayscale image with *N* gray levels has a grayscale cooccurrence matrix with dimensions of $N \times N$. Therefore, if a color image has *N* levels per pixel color component, the CCM would be $N^3 \times N^3$. The size of this matrix makes color quantization necessary. One way to maintain fidelity after color quantization is to use color clustering in a UCS.

In the proposed CCM, the co-occurrence of the most representative colors (centroids after the color quantization) present in an image is analyzed. In this way, P_{ij} or probability of co-occurrence of color index *i* and color index *j* is estimated. For each relative position, a CCM of dimensions $K \times K$ is computed, where *K* is the number of color centroids.

Computation of the CCM features

After computing CCMs, the information contained within them must be summarized into CCM features that can describe texture characteristics. In GLCM, the formulas used to compute these features are based on the difference in matrix indexes. In contrast, this work proposes basing the computation on perceptual differences between colors.

In other words, rather than calculating differences such as $|i-j|$, where *i* and *j* are the color indexes of the quantized image, the color difference, ΔE, between the color with index *i*, $\boldsymbol{C}_i$, and the color with index *j*, $\boldsymbol{C}_j$, is calculated (see Eq. (5)).

The new CCM features are as follows:

a) Homogeneity: $H = \sum_{i,j}^{K,K} \frac{P_{ij}}{1+(\Delta E(\boldsymbol{C}_i,\boldsymbol{C}_j))^2}$ (6)

b) Mean: $\boldsymbol{\mu} = \sum_{i,j}^{K,K} \boldsymbol{C}_i P_{ij}$ (7)

c) Variance: $\sigma^2 = \sum_{i,j}^{K,K} (\Delta E(\boldsymbol{C}_i, \boldsymbol{\mu}_i))^2 P_{ij}$ (8)

d) Correlation: $\rho = \sum_{i,j}^{K,K} \frac{\Delta E(\boldsymbol{C}_i,\boldsymbol{\mu}_i)\Delta E(\boldsymbol{C}_j,\boldsymbol{\mu}_j)}{\sqrt{\sigma_i^2\sigma_j^2}} P_{ij}$ (9)

e) Entropy: $S = \sum_{i,j}^{K,K} -P_{ij}\ln(P_{ij})$ (10)

Experimental Results: Biomedical Applications

The proposed CCM features have been tested with two different applications.

CCM features to detect BCC dermoscopic patterns

First, the capability of CCM features to analyze colored textures was tested in the context of pattern analysis to diagnose skin lesions [10]. To this end, a database was compiled over the course of nine months from Basal Cell Carcinoma (BCC)-diagnosed images received via teledermatology at the Hospital Universitario Virgen Macarena de Sevilla (Spain). All of these dermoscopic images were taken under controlled white LED polarized illumination. However, the brand and specific technical characteristics of the dermatoscopes may vary depending on the local medical center that sent the images. An example of DermLite II Pro dermatoscope (3Gen Inc, San Juan Capistrano, CA), and an example of a dermoscopic image received via Telederma are shown in Figure 2. According to Hanton et al. Color Correlated Temperature (CCT) of usual dermatoscopes varied between 5335° K and 7564° K [11]. In the Color Appearance Model computation, in order to facilitate the automatization of the process, the variables of the CIECAM16 model were chosen as: surround illumination as *average*, L_A=15, Y_b= 20, (X_w, Y_w, Z_w) = (95.05, 100, 108.88), corresponding to the standard illuminant D65 [12].

(a) (b)

Figure 2: Example of: (a) Acquisition device; (b) Dermoscopic image.

All the BCC images used for evaluation were excised and biopsied. Three dermatologists cropped and labeled these images according to one of six possible BCC dermoscopic patterns: ulceration, ovoid nest, multi-globules, maple leaf, spoke wheel, and arborizing telangiectasia. Each image was cropped to 256×256 pixels. More than one pattern may appear in each cropped image. Examples of the six possible BCC dermoscopic patterns are shown in Figure 3. In total, in the database, there are 692 BCCs and 671 non-BCC images, with their dermoscopic pattern annotations.

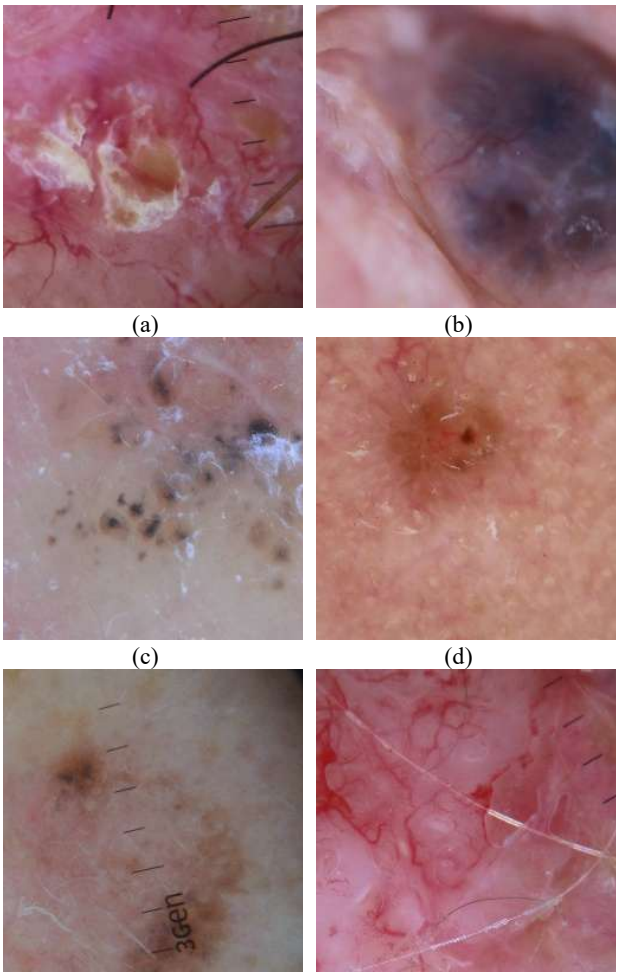

Figure 3: Examples of cropped images showing the six BCC dermatoscopic patterns: (a) ulceration; (b) blue-gray ovoid nest; (c) multi-globules; (d) maple leaf; (e) spoke-wheel; (f) arborizing telangiectasia.

A Deep Neural Network (DNN) was originally trained to detect these six pattens. This DNN has a dual input: the *RGB* image and a color quantized image. This color quantization is performed in CIECAM16 UCS, and then, the quantized image is converted back to the RGB color space. Each input feeds the convolutional layers of a VGG16 neural network, pre-trained with ImageNet. Both outputs are combined with Fully Connected Layers (FCLs). The number of neurons of these FCLs has been optimized to obtain the best classification results. Results obtained by this DNN are shown in Table I (first block)

To evaluate the discriminant power of the proposed CCM features over the deep features automatically learnt by the dual DNN, this DNN model was enhanced with an additional Machine Learning (ML) module (Figure 4). Two experiments were performed. In the first one the inputs to the ML module are traditional GLCM features extracted from L^* component in *CIE* 1976 $L^*a^*b^*$ color space. Results are shown in the second block of Table I. In the second experiment, the proposed CCM features in *CIECAM16* were the inputs to that ML module. The results are shown in the third block of Table I.

As can be observed in this table, the architecture with *CIECAM16* CCM input features outperforms the other two architectures in almost all metrics and patterns. Similarly, *CIECAM16* CCM increases sensitivity by 8% compared to GLCM and improves specificity. These results prove that CCM features provide additional information not contained in the deep features learned by the DNN.

Table I: Performance of AI models (Deep Neural Network) that detects BCC dermoscopic features when incorporating co-occurrence matrix information. PN: Pigment Network (negative criterion); UL: Ulceration; ON: Ovoid Nest; MG: Multi-globules; ML: Maple Leaf; SW: Spoke Wheel; and AT: Arborizing Telangiectasia.

AI model	Derm. Features	SPEC	SENS	AUC
Dual DNN	PN	0.95	0.96	0.98
	AT	0.75	0.87	0.88
	ON	0.71	0.76	0.80
	ML	0.69	0.78	0.83
	UL	0.86	0.79	0.92
	SW	0.80	0.61	0.78
	MG	0.65	0.72	0.77
	Average	**0.78**	**0.78**	**0.85**
Dual DNN + GLCM L^*	PN	0.97	0.97	0.98
	AT	0.73	0.79	0.89
	ON	0.60	0.88	0.79
	ML	0.80	0.77	0.85
	UL	0.76	0.81	0.87
	SW	0.79	0.71	0.89
	MG	0.78	0.79	0.86
	Average	**0.78**	**0.82**	**0.88**
Dual DNN + CIECAM16 CCM	PN	0.98	0.97	0.99
	AT	0.68	0.99	0.91
	ON	0.85	0.83	0.91
	ML	0.72	0.82	0.82
	UL	0.86	0.92	0.94
	SW	0.87	0.93	0.96
	MG	0.79	0.87	0.89
	Average	**0.82**	**0.90**	**0.92**

CCM features to evaluate hemangioma depth

For this experiment, a dermatologist from Hospital Universitario Virgen del Rocío de Sevilla (Spain) compiled and classified a database of infantile hemangiomas (IH). Registering visual and infrared images of the lesions, hemangiomas were roughly segmented. The database contains 82 IH images: 43 superficial ones and 39 deep ones. The images were taken with an in-house camera equipped with an 8-megapixel Sony IMX219 sensor [13]. Examples of superficial and deep IHs are shown in Figure 5. All the images were captured in a consultation room under indoor lighting provided by a light-emitting diode (LED) lamp, which exhibited an approximately Lambertian irradiance

spectrum profile within the visible spectrum. The average room illuminance was 600 lux [14].

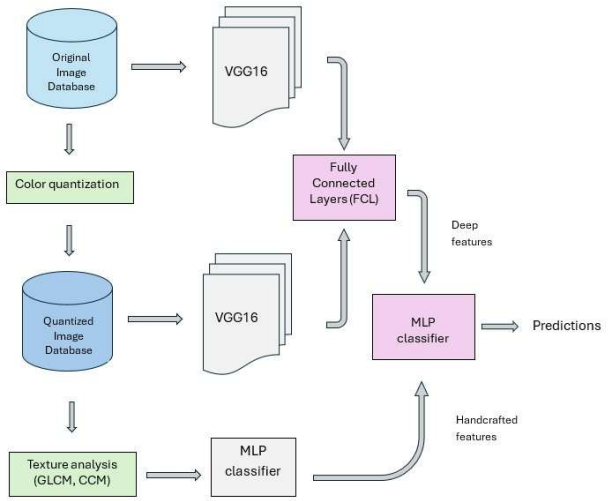

Figure 4: Description of the methodology followed to detect BCC dermoscopic patterns.

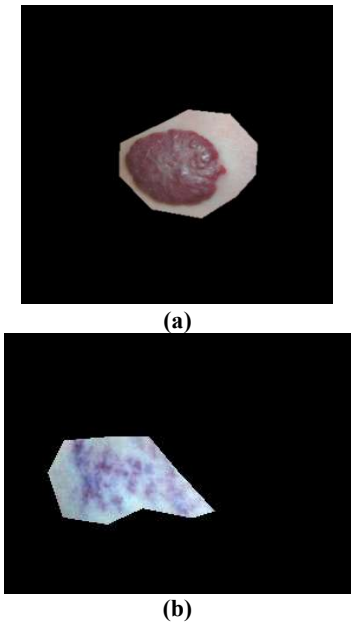

Figure 5: Examples of (a) superficial IH and (b) deep IH

RGB color images were converted to *CIECAM16-UCS* and, subsequently, they were quantized to K=20 representative colors. Thus, 20×20 Color Co-ocurrence Matrices were obtained.

The relative positions between pair of pixels, i.e., the distances and angles that were used to compute the CCM matrices were: 4 angles {0, π/4, π/2, -π/4} and 5 distances {5, 7, 9, 11, 13}. Therefore, we will have a total of 20 CCM matrices per image. From each of these 20 CCM matrices, the 5 features (Eq. 6 to 10) were extracted: homogeneity, variance, entropy, correlation and mean color (which is 3-dimensional vector).

Finally, a feature selection step was applied to determine which features were able to classify IH as superficial or deep. To this end, firstly we calculated the p-value of the five proposed CCM features for the 20 CCM matrices. We found that CCM mean, $\boldsymbol{\mu} = [\bar{J}, \bar{a}, \bar{b}]$, were statistically significant for classifying IH depth, regardless of the angle or distance between pixels. These results are summarized in Table II. This table shows the number of CCM matrices for which each of the five CCM features has a p-value < 0.01.

Table II: Number of CCM matrices where each CCM feature gets a *p*-value<0.01

Homogeneity	0
Mean ($\boldsymbol{\mu}$)	20
Variance	0
Entropy	0
Correlation	0

To further reduce the number of features in the classifier input and analyze the significance of each CCM feature in hemangioma classification, the correlation between features was examined. The results were that the CCM feature **μ**.was correlated for the 20 CCM matrices. The first conclusion that can be drawn from these results is that the information contained in matrices with different angles and distances is the same for this application. This can be understood by observing that these images have no clear directed patterns, but rather a clear predominance of low-frequency-colored patterns.

In view of these results, feature vector **μ** obtained from the CCM matrix where it had lower p-value was selected as input to a classifier. For an additional comparison, the image averages of the six CIECAM16 color correlates [6] were also introduced as inputs of the classifier. The classifier was a Support Vector Machine (SVM). 5-fold cross validation was applied.

The results of this comparison are presented in Table III. The results show that CCM features are the best for this classification problem. Apparently, it appears that color average features alone, **μ**., are sufficient for distinguishing between deep and superficial hemangiomas. But this table shows that the classifier achieves the best results when the average is computed vectorially, and vectorial probability distributions are considered.

Table III: Classification results for different CIECAM16 features as inputs.

	SEN	VPP	Pres	Esp
CIECAM16 correlates	100%	80%	87.5%	75%
Selected CCM feature(**μ**)	100%	100%	100%	100%
Both	87.5%	70%	75%	62.5%

Discussion

New CCM features have been proposed for analyzing colored textures. Calculating these features requires perceptual color clustering and new computational metrics based on perceptual color differences. The usefulness of these CCM features has been validated in two biomedical applications. Further validation should be performed using a general-purpose colored texture database.

Acknowledgements

This research was funded by the grants PROYEXCEL_00889 from the Andalusian Regional Government, and by Grant PID2021-127871OB-I00 funded by MCIN/AEI/10.13039/501100011033 and by "ERDF A way of making Europe".

The authors thank both Dermatology Services at Hospital Universitario Virgen del Rocío de Sevilla (Spain) and Hospital Universitario Virgen Macarena de Sevilla (Spain) for providing the databases used in this research.

References

[1] Anne Humeau-Heurtier, "Color Texture Analysis: a Survey". IEEE Access, 10 (2022).

[2] J. Chaki, N. Dey, "Other Image Color Features" in *Image Color Feature Extraction Techniques*, SpringerBriefs in Computational Intelligence (2021).

[3] S. Shim, T. Choi, Image indexing by modified color co-occurrence matrix, Proc. Internat. Cong. On Image Processing, pp. 14-17 (2003).

[4] A. Vadivel, S. Sural, A.K. Majumdar, "An Integrated Color and Intensity Co-occurrence Matrix", Pattern Recognition Letters, 28 (2007).

[5] R. M. Rangayyan, B. Acha, C. Serrano, Color Image Processing with Biomedical Applications. Society of Photo-Optical Instrumentation Engineers (SPIE), Bellingham, Washington USA (2011).

[6] C. Li, Z. Li, Z. Wang, Y. Xu, M.R. Luo, G. Cui, M. Melgosa, M.H. Brill, M. Pointer, "Comprehensive color solutions: CAM16, CAT16 and CAM16-UCS". Color. Res. Appl., vol. 42, pp. 703–718 (2017).

[7] S.P. Lloyd, "Least squares quantization in PCM". IEEE Trans. Inf. Theory. 28, pp. 29-137 (1982).

[8] R.M. Haralick, K. Shanmugam, I. Dinstein, "Textural Features for Image Classification". IEEE Transactions on Systems, Man, and Cybernetics, 3(6), pp. 610-621 (1973).

[9] E. Cernadas, M. Fernández-Delgado, E. González-Rufino, P. Carrión, "Influence of normalization and color space to color texture classification". Pattern Recognit. 61, pp. 120-138 (2017).

[10] C. Serrano, M. Lazo, A. Serrano, T. Toledo-Pastrana, R. Barros-Tornay, B. Acha, "Clinically Inspired Skin Lesion Classification through the Detection of Dermoscopic Criteria for Basal Cell Carcinoma". Journal of Imaging, 8(7), pp. 197 (2022).

[11] K.L. Hanlon, G, Wei, L. Correa-Selm, J.M. Grichnik, "Dermoscopy and skin imaging light sources: a comparison and review of spectral power distribution and color consistency". J Biomed Opt. 27(8):080902 (2022).

[12] M.R. Luo, M. Pointer. "CIE colour appearance models: A current perspective". Lighting Research & Technology, 50(1):129-140 (2018).

[13] J.A. Leñero-Bardallo, B. Acha, C. Serrano, J.A. Pérez-Carrasco, J. Ortiz-Álvarez, J. Bernabéu-Wittel, "Thermography as a Method for Bedside Monitoring of Infantile Hemangiomas". Cancers, 14, pp. 5392 (2022).

[14] J.A. Pérez-Carrasco, C. Serrano, J.A. Leñero-Bardallo, J. Bernabeu-Wittel, B. Acha, "Advancing infantile hemangioma diagnosis by integrating temperature, color, and texture," J. Biomed. Opt. 30(7) 075001 (2025).